

## Keywords

Image Transmission,  
DST,  
DCT,  
DFT,  
OFDMA,  
PSNR,  
MSE

Received: January 15, 2018

Accepted: February 11, 2018

Published: March 23, 2018

# Wireless Image Transmissions over Frequency Selective Channel Using Recent OFDMA Systems

Faisal Saif Al-kamali, Farouk Abdu Al-fuhaidy,  
Khaled Abdullah Al-soufy

Department of Electrical, Faculty of Engineering and Architecture, IBB University, IBB, Yemen

## Email address

faisalalkamali@yahoo.com (F. S. Al-kamali)

## Citation

Faisal Saif Al-kamali, Farouk Abdu Al-fuhaidy, Khaled Abdullah Al-soufy. Wireless Image Transmissions over Frequency Selective Channel Using Recent OFDMA Systems. *American Journal of Computation, Communication and Control*. Vol. 5, No. 1, 2018, pp. 30-38.

## Abstract

Orthogonal frequency division multiple access (OFDMA) is currently attracting much attention in recent wireless communications to meet the increasing demands arising from the explosive growth of Internet, multimedia and broadband services. In this paper, the issue of the wireless image transmission over OFDMA is investigated for different basis functions, different modulation schemes and different subcarriers mapping schemes over a frequency selective channel. Simulation results show that efficient wireless image transmission over OFDMA is possible for different basis functions. Results also show that the discrete cosine transform (DCT)-based OFDMA (DCT-OFDMA) and discrete sine transform (DST)-based OFDMA (DST-OFDMA) system provide better performance than the conventional discrete Fourier transform (DFT)-based OFDMA (DFT-OFDMA) system. It is found that the interleaved systems greatly enhance the clarity of the received image and their performances are better than that of the localized systems.

## 1. Introduction

The demand for multimedia wireless communications is growing today at an extremely rapid pace and this trend is expected to continue in the future. The common feature of many current wireless standards for high-rate multimedia transmission is the adoption of a multicarrier air interface based on OFDMA. The idea behind OFDMA is to convert a frequency selective channel into a collection of frequency-flat subchannels with partially overlapping spectra. Recently, OFDMA has attracted vast research attention from both academia and industry and has become part of new emerging standards for broadband wireless access. It has been adopted in 3GPP LTE as a downlink scheme and WiMax [1].

In OFDMA systems, the available subcarriers are divided into several mutually exclusive clusters (subchannels or subbands) that are assigned to distinct users for simultaneous transmission. The orthogonality among subcarriers guarantees intrinsic protection against multiple access interference (MAI) while the adoption of a dynamic subcarrier assignment strategy provides the system with high flexibility in resource management. Furthermore, OFDMA inherits from OFDM the ability to compensate channel distortions in the frequency domain without the need of computationally demanding time domain equalizers.

Due to internet growth, wireless transmission of images and video can be easily performed over multipath channels. Image transmission over multicarrier code division multiple access (MC-CDMA), orthogonal frequency division multiplexing (OFDM)

systems and OFDMA has attracted much attentions in the literature [2-8]. However, to the best of the authors' knowledge, the issue of image transmission over OFDMA systems is only considered with the discrete Fourier transform based-OFDMA (DFT-OFDMA) and has not been adequately reported for the discrete cosine transform based-OFDMA (DCT-OFDMA) and the discrete sine transform based-OFDMA (DST-OFDMA), which is the main objective of this paper. In [2, 3], the issue of image transmission over DFT-based MC-CDMA system was studied. Performance evaluation of image transmission over MC-CDMA system using two interleaving schemes was presented in [2]. In [3], an efficient wireless transmission scheme based on the DST-based MC-CDMA system was proposed. Image transmission over a space-time coded OFDM system was suggested and discussed in [4, 5]. Chaotic interleaving for robust image transmission with LDPC coded OFDM was proposed in [6]. Recently, Image transmission over OFDMA and SC-FDMA was reported in [7, 8].

The main objective of this paper is to investigate the issue of wireless image transmission over DFT-OFDMA, DCT-OFDMA and DST-OFDMA systems for different modulation and subcarriers mapping schemes. In this paper, the DFT-OFDMA, the DCT-OFDMA and the DST-OFDMA system models are derived. In addition, the peak-signal-to-noise-ratio (PSNR) and the mean square error (MSE) performances of the received image over DFT-OFDMA, DCT-OFDMA and DST-OFDMA systems are studied, compared and investigated for different modulation and subcarriers mapping schemes.

This paper is organized as follows. In Section II, the basis functions are described. In Section III, the OFDMA system models for different basis functions are derived and presented. In this Section, the complexity of the OFDMA system with different basis functions is investigated and compared. Computer simulation results are given in Section IV for multipath channel environments. Finally, the conclusion of this paper is presented in Section V.

## 2. Basis Functions

The transform operation is mathematical operation that is

$$X(k) = \sqrt{\frac{2}{N}} \beta(k) \sum_{n=0}^{N-1} x(n) \left( \cos \frac{\pi k(2n+1)}{2N} \right), k = 0, 1, \dots, N-1 \quad (4)$$

Where  $x(k)$  is the  $n^{\text{th}}$  sample of the input signal.  $\beta(k)$  can be given as what follows [9]:

$$\beta(k) = \begin{cases} \frac{1}{\sqrt{2}}, & k = 0 \\ 1, & k = 0, 1, \dots, N-1 \end{cases} \quad (5)$$

### 2.3. The Discrete Sine Transform

Like any Fourier-related transform, DST expresses the input signal in terms of a sum of sinusoids with different frequencies and amplitudes. However, it uses only real functions instead of the complex functions used in the

applied to a given signal to convert it from one domain into another domain and vice versa. It is desired to convert the input signal from discrete-time data representation into a discrete-frequency representation and vice versa. Thus once the signal is converted into frequency domain, it will have various components that can be used to remove specific unwanted frequency components. The most popular transform systems related to signal processing are DFT, DST, and DST.

### 2.1. The Discrete Fourier Transform

The DFT is one of the most important tools that is widely used in Digital Signal Processing and related fields. The forward Fourier transform is defined as the integral:

$$X(f) = \int_{-\infty}^{\infty} x(t) e^{-j2\pi Ft} dt \quad (1)$$

The DFT takes  $N$  samples in the time-domain and transforms them into  $N$  values  $X(k)$  in the frequency-domain. It means that DFT operates at a finite number of discrete data points. Thus eq. (1) becomes:

$$X(k) = \sum_{n=0}^{N-1} x(n) \cdot e^{j\frac{2\pi kn}{N}}, k = 0, 1, \dots, N-1 \quad (2)$$

By using Euler's formula than eq. (2) can be rewritten as:

$$X(k) = \sum_{n=0}^{N-1} x(n) \cdot \left( \cos \frac{2\pi nk}{N} - j \sin \frac{2\pi nk}{N} \right) \quad (3)$$

It is clear that DFT takes two parts, real part and imaginary part.

### 2.2. The Discrete Cosine Transform

The DCT is similar to DFT except in the fact that it exploits only the real part of DFT. It expresses the samples of the input signal as the sum of cosinusoidal functions oscillating at different frequencies. There are four types of DCT, however, the type-II DCT is the most commonly used and often called simply the DCT. DCT is given by [9]:

conventional DFT. There are many types of DST and DST-I type is considered in this paper. DST can be expressed by [10]:

$$y(k) = \sum_{n=1}^N X(n) \sin \left( \frac{\pi kn}{N+1} \right), k = 1, 2, \dots, N \quad (6)$$

## 3. OFDMA Systems Models

### 3.1. DFT-OFDMA System

In this subsection, DFT-OFDMA system is considered

with  $U$  users (terminals) communicating at the same time with a fixed base station through independent multipath Rayleigh-fading channels as shown in Figure 1.

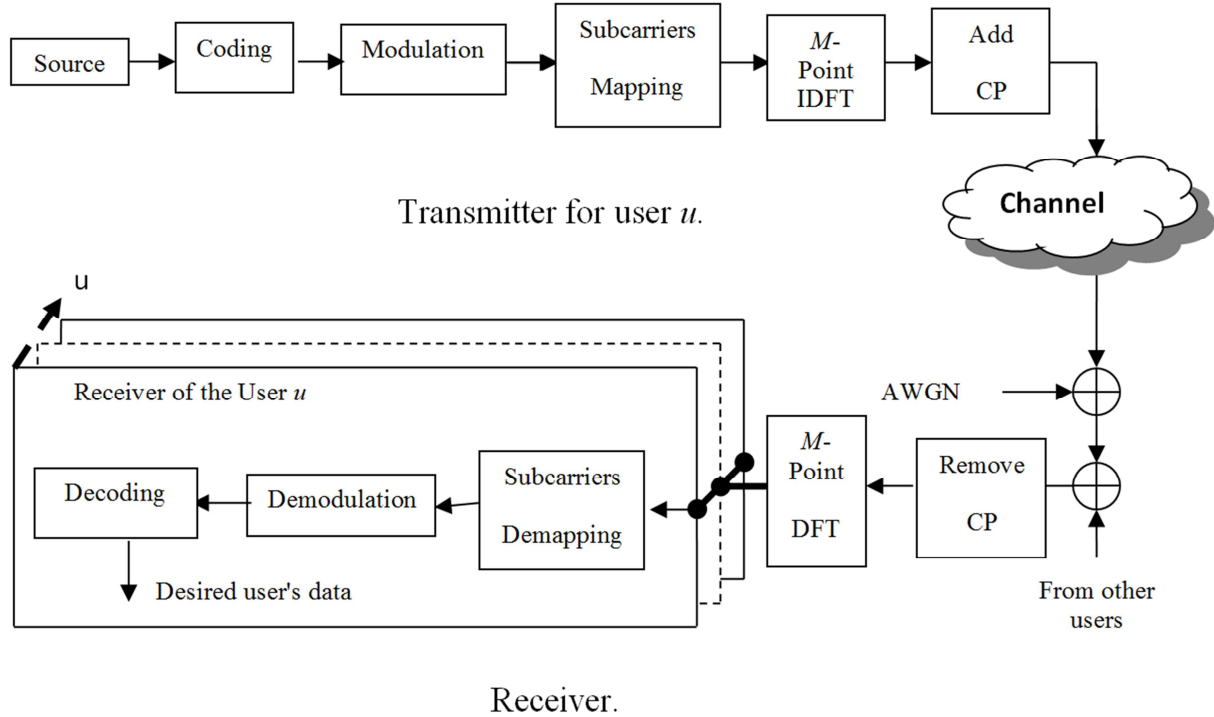


Figure 1. Structure of the uplink DFT-OFDMA system.

At the transmitter of the DFT-OFDMA system, the data symbols are mapped, using the interleaved or the localized subcarriers mapping technique, which enables DFT-OFDMA modulation. Then, an  $M$ -point inverse discrete Fourier transform (IDFT) is performed and a cyclic prefix (CP) is added to the resulting signal. The transmitted signal from the  $u^{th}$  user can be formulated as follows:

$$\bar{\mathbf{x}}^u = \mathbf{P}_{add} \mathbf{F}_M^{-1} \mathbf{M}_T^u \mathbf{d}^u \quad (7)$$

where is an  $N \times 1$  vector containing the modulated symbols of the  $u^{th}$  ( $u=1,2,\dots, U$ ) user.  $\mathbf{M}_T^u$  is an  $M \times N$  ( $M = Q \cdot N$ ) subcarriers mapping matrix of the  $u^{th}$  user.  $Q$  is the bandwidth expansion factor of the symbol sequence. For perfect time and frequency synchronization, if all terminals transmit  $N$  symbols per block, the system can handle  $Q$  simultaneous transmissions without MAI interference.  $\mathbf{F}_M^{-1}$  is the  $M \times M$  IDFT matrix. The generic  $N$ -point DFT matrix

has entries  $[\mathbf{F}_M]_{p,q} = \frac{1}{\sqrt{M}} e^{-j2\pi \frac{pq}{M}}$ , and its inverse is

$\mathbf{F}_M^{-1} = \mathbf{F}_M^H \cdot \mathbf{P}_{add}$  is an  $(M+N_C) \times M$  matrix, which adds a CP of length  $N_C$ .  $\mathbf{P}_{add}$  can be represented as follows:

$$\mathbf{P}_{add} = [\mathbf{C}, \mathbf{I}_M]^T \quad (8)$$

where

$$\mathbf{C} = [\mathbf{0}_{N_C \times (M-N_C)}, \mathbf{I}_{N_C}]^T \quad (9)$$

At the receiver side, assuming perfect time and frequency synchronization, the received signal at the base station can be written as follows:

$$\bar{\mathbf{r}} = \sum_{u=1}^U \mathbf{H}^u \bar{\mathbf{x}}^u + \bar{\mathbf{n}} \quad (10)$$

Where  $\mathbf{H}^u$  is an  $(M+N_C) \times (M+N_C)$  matrix describing the channel of the  $u^{th}$  user.  $\bar{\mathbf{x}}^u$  is an  $(M+N_C) \times 1$  vector containing the transmitted samples of the  $u^{th}$  user.  $\bar{\mathbf{n}}$  is an  $(M+N_C) \times 1$  vector containing the noise. After the removal of the CP, the received signal becomes:

$$\mathbf{r} = \mathbf{P}_{rem} \bar{\mathbf{r}} = \sum_{u=1}^U \mathbf{H}_C^u \tilde{\mathbf{x}}^u + \mathbf{n} \quad (11)$$

where  $\mathbf{P}_{rem}$  is an  $M \times (M+N_C)$  matrix, which removes the CP.  $\mathbf{n} = \mathbf{P}_{rem} \bar{\mathbf{n}}$  and  $\tilde{\mathbf{x}}^u = \mathbf{P}_{rem} \bar{\mathbf{x}}^u$  are the noise and the transmitted signal after the CP removal, respectively.  $\mathbf{H}_C^u$  is an  $M \times M$  circulant matrix describing the channel of the  $u^{th}$  user.  $\mathbf{P}_{rem}$  is given by:

$$\mathbf{P}_{rem} = [\mathbf{0}_{(M \times N_C)}, \mathbf{I}_M] \quad (12)$$

After that, the received signal is transformed into the frequency domain via an  $M$ -points DFT as follows:

$$\mathbf{R} = \sum_{u=1}^U \Lambda^u \bar{\mathbf{X}}^u + \mathbf{N} \quad (13)$$

where  $\bar{\mathbf{X}}^u = \mathbf{F}_M \tilde{\mathbf{x}}^u$  is an  $M \times 1$  vector representing the transmitted samples from the  $u^{th}$  user after the mapping process.  $\mathbf{N}$  is the DFT of  $\mathbf{n}$ . After the demapping process, and the equalization are applied. Finally, the demodulation

and the decoding processes take place.

### 3.2. DCT-OFDMA System

The structure of the DCT-OFDMA system is shown in Figure 2. In matrix notation, the transmitted signal of the  $u^{th}$  user ( $u = 1, 2, \dots, U$ ) can be formulated as follows:

$$\bar{\mathbf{x}}^u = \mathbf{P}_{add} \mathbf{D}_M^{-1} \mathbf{M}_T^u \mathbf{d}^u \quad (14)$$

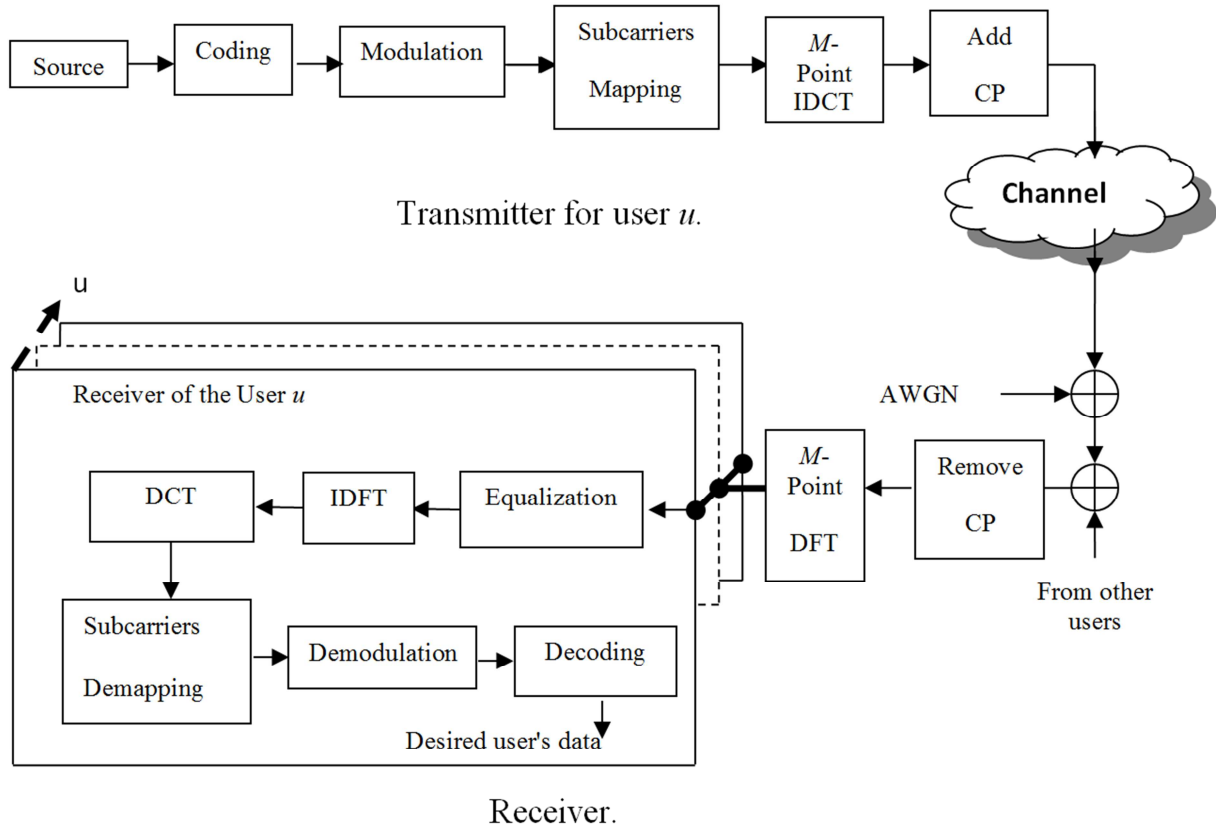


Figure 2. Structure of the uplink DCT-OFDMA system.

where  $\mathbf{D}_M^{-1}$  is an  $M \times M$  IDCT matrix.

At the receiver side, the CP is removed from the received signal and the received signal can be written as follows:

$$\mathbf{r} = \sum_{u=1}^U \mathbf{H}_C^u \tilde{\mathbf{x}}^u + \mathbf{n} \quad (15)$$

where  $\tilde{\mathbf{x}}^u = \mathbf{D}_M^{-1} \mathbf{M}_T^u \mathbf{d}^u$   $\tilde{\mathbf{x}}_u$  is an  $M \times 1$  vector representing the block of the transmitted symbols of the  $u^{th}$  user. Applying the DFT, the received signal can be given by:

$$\mathbf{R} = \sum_{u=1}^U \Lambda_u \mathbf{F}_M \tilde{\mathbf{x}}_u + \mathbf{N} \quad (16)$$

where  $\Lambda_u$  is an  $M \times M$  diagonal matrix containing the DFT

of the circulant sequence of  $\mathbf{H}_u$ .

After that, the FDE, the  $M$ -point IDFT, and the DCT-OFDMA demodulation operations are performed to provide the estimate of the modulated symbols as follows:

$$\hat{\mathbf{x}}_u = \mathbf{M}_u^T \mathbf{S}_M \mathbf{F}_M^{-1} \mathbf{W}_u \mathbf{R} \quad (17)$$

where  $\mathbf{W}_u$  is the  $M \times M$  FDE matrix of the  $u^{th}$  user. Finally, the demodulation and the decoding processes are applied.

### 3.3. DST-OFDMA System

The structure of the DST-SC-FDMA system is similar to that of the DCT-SC-FDMA system in previous subsection. The difference is that the DCT and the IDCT blocks at the transmitter and receiver are replaced by the DST and the

IDST blocks, respectively.

In this paper, the interleaved DFT-OFDMA is denoted by DFT-IOFDMA, the localized DFT-OFDMA is denoted by DFT-LOFDMA, the interleaved DCT-OFDMA is denoted by DCT-IOFDMA, the localized DCT-OFDMA is denoted by DCT-LOFDMA, the interleaved DST-OFDMA is denoted by DST-IOFDMA, and the localized DST-OFDMA is denoted by DST-LOFDMA.

### 4. Complexity Evaluation

At the transmitter of all systems, which is the mobile unit, the complexities of the two transmitter schemes are comparable. At the receiver, which is the base station, the complexities of the DCT-OFDMA and DST-OFDMA systems are slightly higher than that of the DFT-OFDMA system, because the receivers still uses the DFT and the IDFT for the one-tap frequency domain equalizer. However, the increase in the receiver complexity in the uplink is tolerable considering the advantages of the DCT-OFDMA and DST-OFDMA systems.

### 5. Simulation Results

#### 5.1. Simulation Parameters

MATLAB Simulator is used to examine and evaluate the issue of wireless images transmission over OFDMA system with different basis functions. In the simulated OFDMA system, each user occupies 64 subcarriers. The total number of subcarriers  $M= 256$  and the number of users  $U = 4$ . In each simulation, all subcarriers are assigned among all users according to the subcarriers mapping method used. Quadrature phase shift keying (QPSK) and 16 quadrature amplitude modulation (16QAM) modulation schemes are used to generate a transmitted block for each user. MMSE equalization is assumed. The channel model used for simulations is the vehicular A channel [11]. A convolutional code with memory length seven and octal generator polynomials (133, 171) is chosen as the channel code. The transmitted Lena image for all users of size  $256 \times 256$  is shown in Figure 3. As mentioned earlier, while evaluating the performance of image transmission over OFDMA system with different basis functions, PSNR and MSE metrics are considered.

#### 5.2. PSNR Performance

In this section, the Lena image of size  $256 \times 256$  has been

transmitted over the coded OFDMA systems with different basis functions, the DFT, the DCT and the DST and as well as with different subcarriers mapping schemes and different modulation schemes. The PSNR values of the received image are calculated for different SNR values from 0 through 35 dB in 5 dB steps. The wireless channel used in this paper is the vehicular A channel.



Figure 3. Lena image.

The experimental results are listed in Table 1 and 2 for QPSK and 16QAM modulation schemes and plotted in Figures 4 and 5, respectively.

Figure 4 illustrates the relationship between PSNR and SNR when Lena image is transmitted through the DFT-OFDMA, DST-OFDMA and DCT-OFDMA systems for different subcarriers mapping schemes and the QPSK is used. From the figure, it is observed that as SNR is increased, the PSNR increases.

On the other hand Figure 5 shows the efficiency of image transmission over DFT-OFDMA, DST-OFDMA and DCT-OFDMA with different subcarriers mapping schemes when 16QAM modulation scheme is used.

As shown in the figure, the PSNR for the three systems increases with increasing of SNR.

From these two figures, it is clear that the interleaved systems give the best PSNR performance when compared with the localized systems.

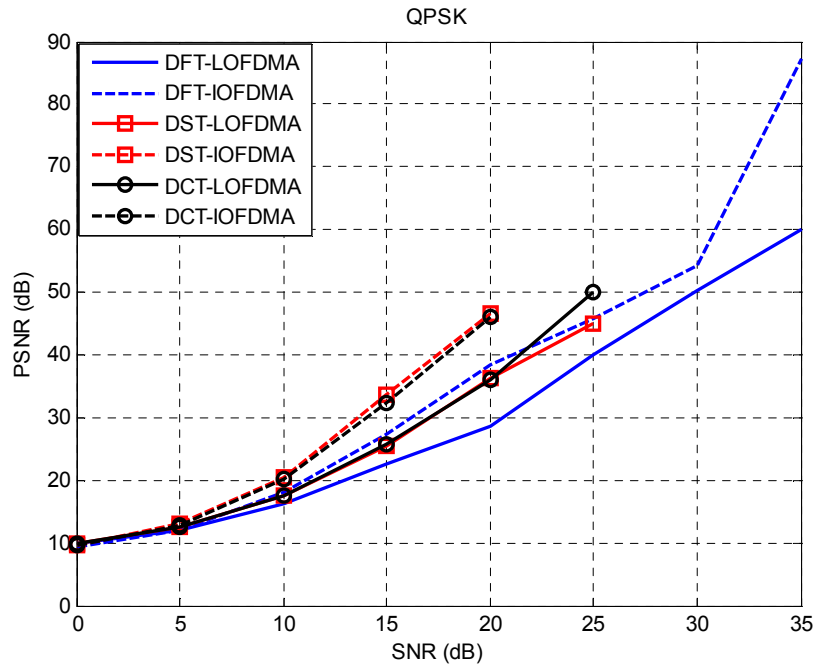
Furthermore, it is also noted that DST-IOFDMA and DCT-IOFDMA systems provide better PSNR performance than DFT-IOFDMA system. More precisely, PSNR performance of DST-IOFDMA is better than DCT-IOFDMA but beyond 20 dB both systems provide the same PSNR performance.

Table 1. PSNR values of the received Lena image over the DFT-OFDMA, the DCT-OFDMA and the DST-OFDMA systems when QPSK is used.

SNR (dB)	DFT-OFDMA		DST-OFDMA		DCT-OFDMA	
	LOFDMA	IOFDMA	LOFDMA	IOFDMA	LOFDMA	IOFDMA
0	9.8115	9.4314	9.8626	9.7615	9.7787	9.6499
5	12.1075	12.1275	12.5224	13.0071	12.5083	12.9174
10	16.3071	18.1873	17.6208	20.5690	17.4207	20.2464
15	22.5329	27.3135	25.4493	33.6732	25.6598	32.4304
20	28.6789	38.3529	36.2496	46.5490	36.1430	46.0184
25	39.8665	45.8774	45.0751	Inf	50.0218	Inf
30	50.1585	54.1450	Inf	Inf	Inf	Inf
35	60.1720	87.2647	Inf	Inf	Inf	Inf

**Table 2.** PSNR values of the received Lena image over the DFT-OFDMA, the DCT-OFDMA and the DST-OFDMA systems when 16QAM is used.

SNR (dB)	DFT-OFDMA		DST-OFDMA		DCT-OFDMA	
	LOFDMA	IOFDMA	LOFDMA	IOFDMA	LOFDMA	IOFDMA
0	8.8450	8.6802	8.7749	8.7263	8.7373	8.7107
5	10.1244	9.1684	9.8894	9.2229	9.7565	9.1344
10	12.7598	11.7093	12.6334	11.6836	12.4601	11.5742
15	16.3857	16.1536	15.9924	16.0386	15.8206	16.0151
20	21.5065	24.3564	21.3454	23.5050	21.2758	23.4926
25	26.8155	33.7903	28.2985	33.8133	28.5680	33.3724
30	34.3729	44.6174	36.9373	46.1578	39.0653	42.5203
35	42.8777	51.1363	46.8410	59.1490	54.3258	60.1382



**Figure 4.** PSNR against SNR of the Lena image transmission over the DFT-OFDMA, the DCT-OFDMA and the DST-OFDMA systems when the QPSK is used.

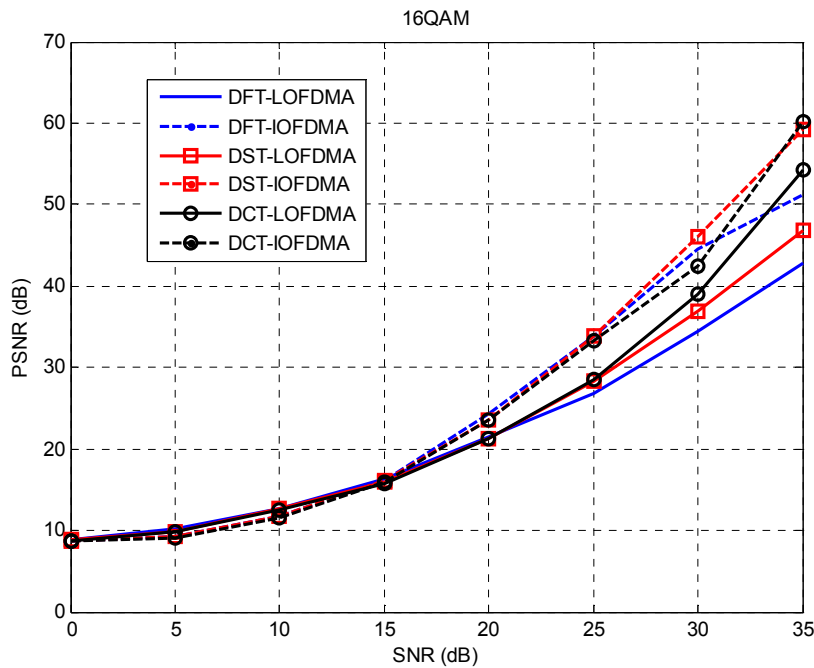


**Figure 5.** PSNR against SNR of the Lena image transmission over the DFT-OFDMA, the DCT-OFDMA and the DST-OFDMA systems when the 16QAM is used.

### 5.3. MSE Performance

In this section, several experiments are conducted to test and investigate the MSE performance of the received image over DFT-OFDMA, DST-OFDMA and DCT-OFDMA for different subcarriers mapping schemes when the QPSK and the 16QAM modulation techniques are used. The obtained MSE values are listed in Tables 3 and 4 and plotted in Figures 6 and 7.

**Table 3.** MSE values of the received Lena image over the DFT-OFDMA, the DCT-OFDMA and the DST-OFDMA systems when QPSK is used.

SNR (dB)	DFT-OFDMA		DST-OFDMA		DCT-OFDMA	
	LOFDMA	IOFDMA	LOFDMA	IOFDMA	LOFDMA	IOFDMA
0	0.1044	0.1140	0.1032	0.1056	0.1052	0.1084
5	0.0616	0.0613	0.0559	0.0500	0.0561	0.0511
10	0.0234	0.0152	0.0173	0.0088	0.0181	0.0094
15	0.0056	0.0019	0.0029	4.2922e-004	0.0027	5.7142e-004
20	0.0014	1.4612e-004	2.3716e-004	2.2136e-005	2.4305e-004	2.5013e-005
25	1.0312e-004	2.5838e-005	3.1081e-005	0	9.9498e-006	0
30	9.6417e-006	3.8503e-006	0	0	0	0
35	9.6117e-007	1.8773e-009	0	0	0	0

Figure 6 shows the relation between MSE and SNR when Lena image is transmitted through the DFT-OFDMA, DST-OFDMA and DCT-OFDMA systems for different subcarriers mapping schemes and QPSK modulation scheme is used. It is observed that with increasing SNR, the MSE is decreased.

**Table 4.** MSE values of the received Lena image over the DFT-OFDMA, the DCT-OFDMA and the DST-OFDMA systems when 16QAM is used.

SNR (dB)	DFT-OFDMA		DST-OFDMA		DCT-OFDMA	
	LOFDMA	IOFDMA	LOFDMA	IOFDMA	LOFDMA	IOFDMA
0	0.1305	0.1355	0.1326	0.1341	0.1337	0.1346
5	0.0972	0.1211	0.1026	0.1196	0.1058	0.1221
10	0.0530	0.0675	0.0545	0.0679	0.0568	0.0696
15	0.0230	0.0242	0.0252	0.0249	0.0262	0.0250
20	0.0071	0.0037	0.0073	0.0045	0.0075	0.0045
25	0.0021	4.1780e-004	0.0015	4.1559e-004	0.0014	4.6001e-004
30	3.6535e-004	3.4535e-005	2.0243e-004	2.4222e-005	1.2401e-004	5.5972e-005
35	5.1550e-005	7.6978e-006	2.0697e-005	1.2165e-006	3.6933e-006	9.6868e-007

It is clear that the transmitted image using the DST-OFDMA and DCT-OFDMA systems give lower MSE values than DFT-OFDMA system. Moreover, it is noted that DST-IOFDMA and DCT-IOFDMA have significantly smaller MSE than DFT-IOFDMA.

Same previous scenario is done when 16QMA modulation scheme is used and the results are shown in Figure 7. As shown in the figure, it is observed that DST-IOFDMA and DCT-IOFDMA have significantly smaller MSE than DFT-IOFDMA system.

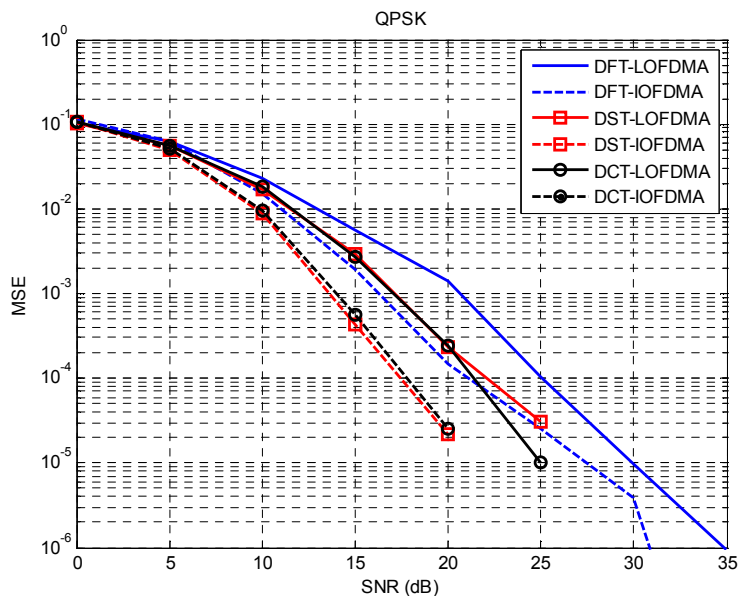


**Figure 6.** MSE versus SNR of the Lena image transmission over the DFT-OFDMA, the DCT-OFDMA and the DST-OFDMA systems when the QPSK is used.

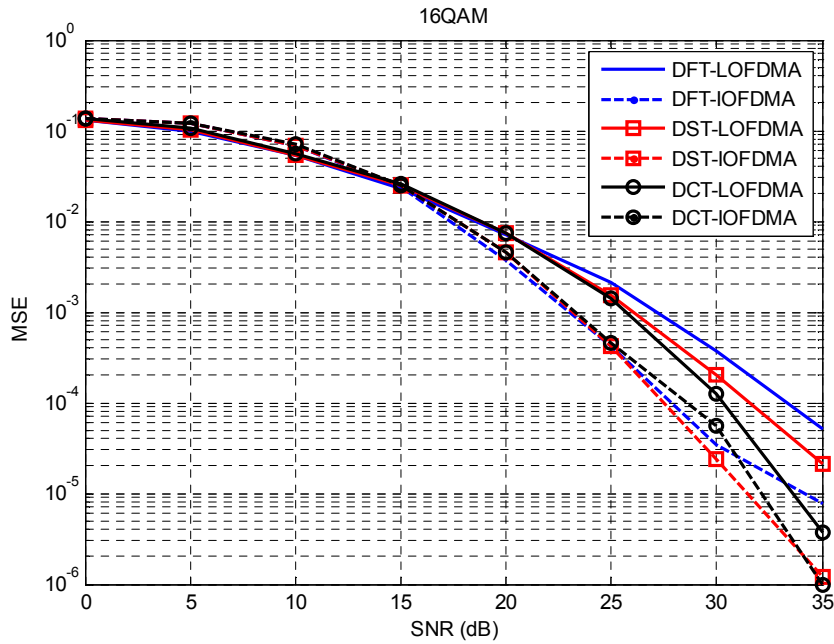


Figure 7. MSE versus SNR of the Lena image transmission over the DFT-OFDMA, the DCT-OFDMA and the DST-OFDMA systems when the 16QAM is used.



Figure 8. Image for different OFDMA Systems at SNR = 20 dB and QPSK.

### 5.4. Clarity Investigation

The visual quality of the reconstructed images at SNR value 15 dB is demonstrated and the received images of one uplink user are shown in Figure 8 for different OFDMA systems. By comparing these received images with the original image in Figure 3, it can conclude the superiority of the DST-OFDMA and DCT-OFDMA system over the conventional DFT-OFDMA system for different subcarriers mapping schemes.

### 6. Conclusion

In this paper, wireless transmission of gray-scale images over OFDMA system is tested for different basis functions, different subcarriers mapping schemes and different modulation schemes. It is shown that transmitting wireless images over OFDMA systems is possible for different basis functions. The obtained results show a noticeable performance improvement for the DST-OFDMA and DCT-OFDMA systems in terms of the MSE and PSNR over the conventional DFT-OFDMA system. On the other hand, transmitting wireless images using the DCT or the DST as the basis function in the OFDMA system greatly enhances the clarity of the received images than that using the DFT as the basis function in the OFDMA system. Moreover, the interleaved scheme provides better MSE and PSNR performances than the localized schemes for all systems, especially with QPSK.

### References

[1] H. G. Myung and D. J. Goodman, Single Carrier FDMA: A New Air Interface for Long Term Evaluation, John Wiley & Sons, Chichester, UK, 2008.

- [2] E. M. El-Bakary, E. S. Hassan, O. Zahran, S. A. El-Dolil, and F. E. Abd El-Samie, "Efficient image transmission with multi-carrier CDMA," *Wireless Personal Communications*, Springer, vol. 69, No. 2, pp. 979-994, March 2013.
- [3] A. F. Al-Junaid and F. S. Al-kamali, "Efficient wireless transmission scheme based on the recent DST-MC-CDMA," *Wireless Networks*, Springer, Vol. 22, No. 3, pp. 813-824, April 2016.
- [4] Y. Sun and Z. Xiong, "Progressive image transmission over space-time coded OFDM-based MIMO systems with adaptive modulation," *IEEE Trans. On Mobile Computing*, vol. 5, No. 8, pp. 1016-1028, 2006.
- [5] M. Shayegannia, A. Hajshirmohammadi, S. Muhaidat and M. Torki, "Space-time coding MIMO-OFDM SAR for high-resolution imaging," *IET Image Processing*, vol. 7, No. 1, pp. 33-41, 2013.
- [6] N. F. Soliman, Y. Albagory, M. A. Elbendary, W. Al-Hanafy, E. M. El-Rabaie, S. A. Alshebeili, and F. E. Abd El-Samie, "Chaotic interleaving for robust image transmission with LDPC coded OFDM," *Wireless Personal Communications*, Vol. 79, No. 3, pp. 2141-2154, Dec. 2014.
- [7] Faisal S. Al-Kamali, Abdullah A. Qasem, "Wireless Images Transmission over OFDMA Systems: Investigation and Evaluation," *IET JOE*. pp. 1-12, 2016.
- [8] F. S. Al-Kamali, A. A. Qasem, S. A. Abuasbaa and G. A. Qasem "SC-FDMA and OFDMA: An Efficient Wireless Image Transmission Schemes," *Journal of Control and Systems Engineering*, Vol. 4, No. 1, pp. 74-83, 2016.
- [9] P. Tan, and N. C. Beaulieu, "A Comparison of DCT-Based OFDM and DFT-Based OFDM in Frequency Offset and Fading Channels," *IEEE Transactions on Communications*, Vol. 54, No. 11, Nov. 2006.
- [10] [http://en.wikipedia.org/wiki/Discrete\\_sine\\_transform](http://en.wikipedia.org/wiki/Discrete_sine_transform), accessed date 15/07/2017s.
- [11] 3rd generation partnership project, 3GPP TS 25.101 – technical specification group radio access network; user equipment (UE) radio transmission and reception (FDD) (Release 7), Section B.2.2, Sep. 2007.

## Biographies



**Faisal Saif Al-kamali** has received the B.Sc. degree in Electronics and Communications Engineering from the Faculty of Engineering, Baghdad University, Baghdad, Iraq, in 2001. He has received the M.Sc., and PhD degrees in Communication Engineering from the Faculty of Electronic Engineering, Menoufia University, Menouf, Egypt, in 2008, and 2011, respectively. He joined the teaching staff of the Department of Electrical, Faculty of Engineering and architecture, Ibb University, Ibb, Yemen in 2011. He has served as a head of the Electrical department, Ibb University from Oct. 2013 to Oct. 2014. He is a co-author of more than 30 papers in national and international conferences and journals and one textbook. His research areas of interest include CDMA Systems, OFDMA Systems, Single Carrier FDMA (SC-FDMA) System, MIMO Systems, Interference Cancellation, Synchronization, Channel Equalization and Channel Estimation.



**Khaled Abdullah Al-soufy**. He received his B.Sc in Computer and control engineering from Sanaa University, Yemen, in 1998. He received his M.Tech in Computer Science and Engineering from Osmania University, Hyderabad, India in 2006. He received his Ph.D. in 2015 from Computer Engineering, from department of computer Engineering, Z. H. College of Engineering and Technology, Aligarh Muslim University, Aligarh, India. He has joined the teaching staff of the Department of Electrical Engineering, Faculty of Engineering and Architecture, Ibb University, Yemen, in 2013. His research interest includes mobile computing and Quality of service in mobile ad hoc networks, Sensor network, wireless network, image and signal processing.



**Farouk Abdu Al-fuhaidy**. He received the B.S.E.E. Computer Engineering and M.S.E.E. in Computer Engineering respectively and Ph.D. in Communication Engineering from the Military Technical College, Cairo, Egypt in 2007, 2009 and 2013 respectively. He joined the teaching staff of the Department of Electrical Engineering, Faculty of Engineering and Architecture, Ibb University, Yemen, in 2014. His research interests and activities are in the areas of Wireless Sensor Networks, Embedded Systems, broadband communications and spread-spectrum communications, advanced signal processing, and image processing.